Triaxial Testing of Soils

Poul V. Lade

WILEY Blackwell

Triaxial Testing of Soils

Triaxial Testing of Soils

Poul V. Lade

WILEY Blackwell

This edition first published 2016

Registered Office
John Wiley & Sons, Ltd, The Atrium, Southern Gate, Chichester, West Sussex, PO19 8SQ, United Kingdom.

Editorial Offices
9600 Garsington Road, Oxford, OX4 2DQ, United Kingdom.
The Atrium, Southern Gate, Chichester, West Sussex, PO19 8SQ, United Kingdom.

For details of our global editorial offices, for customer services and for information about how to apply for permission to reuse the copyright material in this book please see our website at www.wiley.com/wiley-blackwell.

Library of Congress Cataloging-in-Publication data applied for

ISBN: 9781119106623

A catalogue record for this book is available from the British Library.

Wiley also publishes its books in a variety of electronic formats. Some content that appears in print may not be available in electronic books.

Set in 10/12pt Palatino by SPi Global, Pondicherry, India

1 2016

Contents

Preface

The triaxial test is almost always chosen for studies of new phenomena, because it is relatively simple and versatile. The triaxial test is the most suitable for such studies and it is required in geotechnical engineering for the purposes of design of specific projects and for studying and understanding the behavior of soils.

The first triaxial compression test apparatus, shown in Fig. P.1, was designed by von Kārmān (1910, 1911) for testing of rock cores. The scale may be deduced from the fact that the specimen is 4 cm in diameter (Vásárhelyi 2010). However, his paper was not noticed or it was forgotten by 1930 when Casagrande at Harvard University wrote a letter to Terzaghi at the Technical University in Vienna in which he describes his visit to the hydraulics laboratory in Berlin. Here he saw an apparatus for measuring the permeability of soil. Casagrande suggested that the cylindrical specimen in this apparatus could be loaded in the vertical (axial) direction to indicate its strength. Therefore, he was going to build a prototype, and Terzaghi proposed that he build one for him too. This appears to be the beginning of triaxial testing of soils in geotechnical engineering. The apparatus was immediately employed by Rendulic (Terzaghi and Rendulic 1934) for tests with and without membranes, the results of which played an important role in understanding the effective stress principle as well as the role of pore water pressure and consolidation on shear strength at a time when the effective stress principle was still being questioned (Skempton 1960; de Boer 2005).

Previous books on the developments of techniques for triaxial testing have been written by Bishop and Henkel (1957, 1962) and by Head (1986). The proceedings from a conference on Advanced Triaxial Testing of Soil and Rock (Donaghe *et al*. 1988) was published to summarize advances in this area. Other books have not appeared since then. To understand the present book, the reader is required to have a background in basic soil mechanics, some experience in soil mechanics laboratory testing and perhaps in foundation engineering.

In addition to triaxial testing of soils, the contents of the book may in part apply to more advanced tests and to the testing of hard soils – soft rocks. It is written for research workers, soil testing laboratories and consulting engineers. The emphasis is placed on what the soil specimen is exposed to and experiences rather than the esthetic appearance of the equipment. There will be considerable use of physics and mathematics to illustrate the arguments and discussions. With a few exceptions, references are made to easily accessible articles in the literature. Much of the book centers on how to obtain high quality experimental results, and the guiding concepts for this purpose have been expressed by the car industry in their slogans "Quality is Job One" (Ford Motor Company) and "Quality is never an accident, it is always the result of excellent workmanship" (Mercedes).

The book is organized in a logical sequence beginning with the principles of triaxial testing in Chapter 1, and the computations and presentations of test results in Chapter 2. The triaxial equipment is explained in Chapter 3, and instrumentation, measurements, and control is reviewed in Chapter 4. Preparation of triaxial specimens is presented in Chapter 5, and saturation of specimens is described in Chapter 6. The two testing stages in an experiment are made clear in Chapter 7: Consolidation and in Chapter 8: Shearing. Chapter 9 accounts for the corrections to the measurements, Chapter 10 informs about special tests and test conditions, and Chapter 11 puts the results from triaxial tests in perspective by reviewing results from

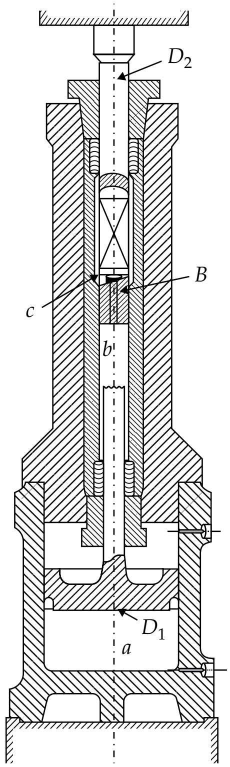

Figure P.1 Triaxial apparatus designed and constructed for testing of rock cores by von Kārmān (1910, 1911).

tests with three unequal principal stresses. Appendices are provided to explain special experimental techniques. Information on vendors for the various types of equipment may be obtained from the internet.

The author's background for writing this book consists of a career in laboratory experimentation at university level to study and model the behavior of soils. More specifically, he received an MS degree in 1967 from the Technical University of Denmark for which he wrote a thesis on the influence of the intermediate principal stress on the strength of sand and, in retrospect, ended up with the wrong conclusion on the basis of perfectly correct results. He received a PhD from the University of California at Berkeley in 1972 with a dissertation on "The Stress–Strain and Strength Characteristics of Cohesionless Soils," which included results from triaxial compression tests, true triaxial tests and torsion shear tests to indicate the effects of the intermediate principal stress on sand behavior, as well as a three-dimensional elasto-plastic constitutive model for the behavior of soils.

With his students, the author developed testing equipment, performed experiments and built constitutive models for the observed soil behavior while a professor at the University of California at Los Angeles (UCLA) (1972–1993), Johns Hopkins University (1993–1999), Aalborg University in Denmark (1999–2003), and the Catholic University of America in Washington, DC (2003–2015). Many of the experimental techniques developed over this range of years are explained in the present book.

Great appreciation is expressed to John F. Peters of the US Army Engineer Research and Development Center in Vicksburg, MS for his careful review of the manuscript and for his many comments. Special thanks go to Afshin Nabili for his invaluable assistance with drafting a large number of the figures and for modification of other diagrams for the book.

Poul V. Lade
October 2015

References

Bishop, A.W. and Henkel, D.J. (1957) *Measurement of Soil Properties in Triaxial Test*. Edward Arnold, London.

Bishop, A.W. and Henkel, D.J. (1962) *The Measurement of Soil Properties in the Triaxial Test*, 2nd edn. St. Martin's Press, New York, NY.

de Boer, R. (2005) *The Engineer and the Scandal*. Springer, Berlin.

Donaghe, R.T., Chaney, R.C., and Silver, M.L. (eds) (1988) *Advanced Triaxial Testing of Soil and Rock, ASTM STP 977*. ASTM, Philadelphia, PA.

Head, K.H. (1986) *Manual of Soil Laboratory Testing – Volume 3: Effective Stress Tests*. Pentech Press, London.

von Kārmān, T. (1910) *Magyar Mérnök és Ėpitészegylet Közlönye*, **10**, 212–226.

von Kārmān, T. (1911) *Verhandlungen Deutsche Ingenieur*, **55**, 1749–1757.

Skempton, A.W. (1960) Terzaghi's discovery of effective stress. In: *From Theory to Practice in Soil Mechanics* (eds L. Bjerrum, A. Casagrande, R.B. Peck and A.W. Skempton), pp. 42–53. John Wiley and Sons, Ltd, London.

Terzaghi, K. and Rendulic, L. (1934) Die wirksame Flächenporosität des Betons. *Zeitschrift des Ōsterreichischen Ingenieur- und Architekten Vereines*, **86**, 1–9.

Vásárhelyi, B. (2010) Tribute to the first triaxial test performed in 1910. *Acta Geology and Geophysics of Hungary*, **45**(2), 227–230.

About the Author

Poul V. Lade received his MS degree from the Technical University of Denmark in 1967 and he continued his studies at the University of California at Berkeley where he received his PhD in 1972. Subsequently his academic career began at the University of California at Los Angeles (UCLA) and he continued at Johns Hopkins University (1993–1999), Aalborg University in Denmark (1999–2003), and the Catholic University of America in Washington, DC (2003–2015).

His research interests include application of appropriate experimental methods to determine the three-dimensional stress–strain and strength behavior of soils and the development of constitutive models for frictional materials such as soils, concrete, and rock. He developed laboratory experimental apparatus to investigate monotonic loading and large three-dimensional stress reversals in plane strain, true triaxial and torsion shear equipment. This also included studies of effects of principal stress rotation, stability, instability and liquefaction of granular materials, and time effects. The constitutive models are based on elasticity and work-hardening, isotropic and kinematic plasticity theories.

He has written nearly 300 publications based on research performed with support from the National Science Foundation (NSF) and from the Air Force Office of Scientific Research (AFOSR). He was elected member of the Danish Academy of Technical Sciences (2001), and he was awarded Professor Ostenfeld's Gold Medal from the Technical University of Denmark (2001). He was inaugural editor of *Geomechanics and Engineering* and he has served on the editorial boards of eight international journals on geotechnical engineering.

1 Principles of Triaxial Testing

1.1 Purpose of triaxial tests

The purpose of performing triaxial tests is to determine the mechanical properties of the soil. It is assumed that the soil specimens to be tested are homogeneous and representative of the material in the field, and that the desired soil properties can in fact be obtained from the triaxial tests, either directly or by interpretation through some theory.

The mechanical properties most often sought from triaxial tests are stress–strain relations, volume change or pore pressure behavior, and shear strength of the soil. Included in the stress–strain behavior are also the compressibility and the value of the coefficient of earth pressure at rest, K_0. Other properties that may be obtained from the triaxial tests, which include time as a component, are the permeability, the coefficient of consolidation, and properties relating to time dependent behavior such as rate effects, creep, and stress relaxation.

It is important that the natural soil deposit or the fill from which soil samples have been taken in the field are sufficiently uniform that the soil samples possess the properties which are appropriate and representative of the soil mass in the field. It is therefore paramount that the geology at the site is well-known and understood. Even then, samples from uniform deposits may not "contain" properties that are representative of the field deposit. This may happen either (a) due to the change in effective stress state which is always associated with the sampling process or (b) due to mechanical disturbance from sampling, transportation, or handling in the laboratory. The stress–strain and strength properties of very sensitive clays which have been disturbed cannot be regenerated in the laboratory or otherwise obtained by interpretation of tests performed on inadequate specimens. The effects of sampling will briefly be discussed below in connection with choice of consolidation pressure in the triaxial test. The topic of sampling is otherwise outside the scope of the present treatment.

1.2 Concept of testing

The concept to be pursued in testing of soils is to simulate as closely as possible the process that goes on in the field. Because there is a large number of variables (e.g., density, water content, degree of saturation, overconsolidation ratio, loading conditions, stress paths) that influence the resulting soil behavior, the simplest and most direct way of obtaining information pertinent to the field conditions is to duplicate these as closely as possible.

Triaxial Testing of Soils, First Edition. Poul V. Lade.

However, because of limitations in equipment and because of practical limitations on the amount of testing that can be performed for each project, it is essential that:

1. The true field loading conditions (including the drainage conditions) are known.
2. The laboratory equipment can reproduce these conditions to a required degree of accuracy.
3. A reasonable estimate can be made of the significance of the differences between the field loading conditions and those that can be produced in the laboratory equipment.

It is clear that the triaxial test in many respects is incapable of simulating several important aspects of field loading conditions. For example, the effects of the intermediate principal stress, the effects of rotation of principal stresses, and the effects of partial drainage during loading in the field cannot be investigated on the basis of the triaxial test. The effects of such conditions require studies involving other types of equipment or analyses of boundary value problems, either by closed form solutions or solutions obtained by numerical techniques.

To provide some background for evaluation of the results of triaxial tests, other types of laboratory shear tests and typical results from such tests are presented in Chapter 11. The relations between the different types of tests are reviewed, and their advantages and limitations are discussed.

1.3 The triaxial test

The triaxial test is most often performed on a cylindrical specimen, as shown in Fig. 1.1(a). Principal stresses are applied to the specimen, as indicated in Fig. 1.1(b). First a confining pressure, σ_3, is applied to the specimen. This pressure acts all around and therefore on all planes in the specimen. Then an additional stress difference, σ_d, is applied in the axial direction. The stress applied externally to the specimen in the axial direction is

$$\sigma_1 = \sigma_d + \sigma_3 \tag{1.1}$$

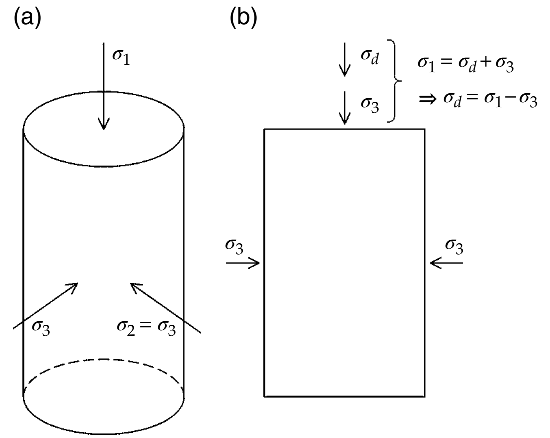

Figure 1.1 (a) Cylindrical specimen for triaxial testing and (b) stresses applied to a triaxial specimen.

and therefore

$$\sigma_d = \sigma_1 - \sigma_3 \tag{1.2}$$

In the general case, three principal stresses, σ_1, σ_2 and σ_3 may act on a soil element in the field. However, only two different principal stresses can be applied to the specimen in the conventional triaxial test. The intermediate principal stress, σ_2, can only have values as follows:

$$\sigma_2 = \sigma_3 : \text{Triaxial compression} \tag{1.3}$$

$$\sigma_2 = \sigma_1 : \text{Triaxial extension} \tag{1.4}$$

The condition of triaxial extension can be achieved by applying negative stress differences to the specimen. This merely produces a reduction in compression in the extension direction, but no tension occurs in the specimen. The state of stress applied to the specimen is in both cases axisymmetric. The triaxial compression test will be discussed in the following, while the triaxial extension test is discussed in Chapter 10.

The test is performed using triaxial apparatus, as seen in the schematic illustration in Fig. 1.2. The specimen is surrounded by a cap and a base and a membrane. This unit is placed in a triaxial cell in which the cell pressure can be applied. The cell pressure acts as a hydrostatic confinement for the specimen, and the pressure is therefore the same in all directions. In addition,

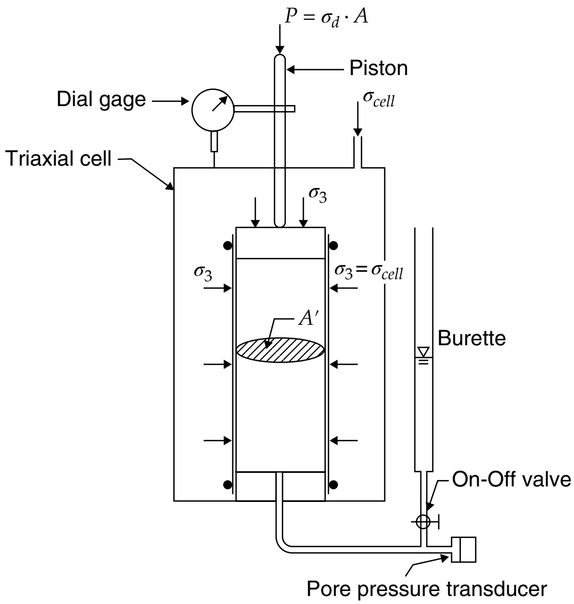

Figure 1.2 Schematic diagram of triaxial apparatus.

a deviator load can be applied through a piston that goes through the top of the cell and loads the specimen in the axial direction.

The vertical deformation of the specimen may be measured by a dial gage attached to the piston which travels the same vertical distance as the cap sitting on top of the specimen. Drainage lines are connected to the water saturated specimen through the base (or both the cap and the base) and connected to a burette outside the triaxial cell. This allows for measurements of the volume changes of the specimen during the test.

Alternatively, the connection to the burette can be shut off thereby preventing the specimen from changing volume. Instead the pore water pressure can be measured on a transducer connected to the drainage line.

The following quantities are measured in a typical triaxial test:

1. Confining pressure
2. Deviator load
3. Vertical (or axial) deformation
4. Volume change or pore water pressure

These measurements constitute the data base from which other quantities can be derived [e.g., stress difference $(\sigma_1 - \sigma_3)$, axial strain ε_1, and volumetric strain ε_v].

1.4 Advantages and limitations

Whereas the triaxial test potentially can provide a substantial proportion of the mechanical properties required for a project, it has limitations, especially when special conditions are encountered and necessitates clarification based on experimentation.

The *advantages* of the triaxial test are:

1. Drainage can be controlled (on–off)
2. Volume change or pore pressure can be measured
3. Suction can be controlled in partially saturated soils
4. Measured deformations allow calculation of strains and moduli
5. A larger variety of stress and strain paths that occur in the field can be applied in the triaxial apparatus than in any other testing apparatus (e.g., initial anisotropic consolidation at any stress ratio including K_0, extension, active and passive shear).

The *limitations* of the triaxial test are:

1. Stress concentrations due to friction between specimen and end plates (cap and base) cause nonuniform strains and stresses and therefore nonuniform stress–strain, volume change, or pore pressure response.
2. Only axisymmetric stress conditions can be applied to the specimen, whereas most field problems involve plane strain or general three-dimensional conditions with rotation of principal stresses.
3. Triaxial tests cannot provide all necessary data required to characterize the behavior of an anisotropic or a cross-anisotropic soil deposit, as illustrated in Fig. 1.3.
4. Although the axisymmetric principal stress condition is limited, it is more difficult to apply proper shear stresses or tension to soil in relatively simple tests.

The first limitation listed above can be overcome by applying lubricated ends on the

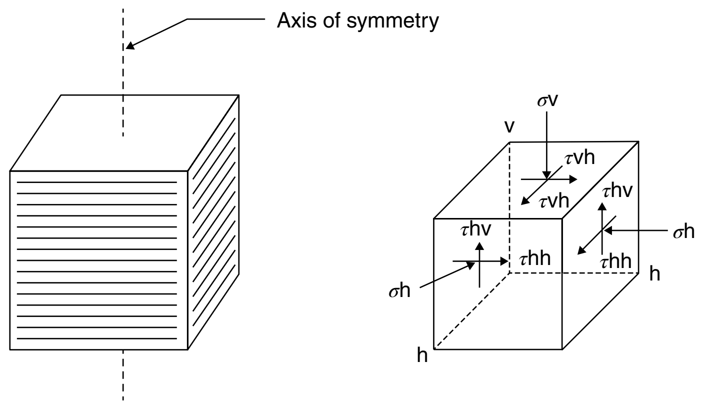

Require tests with application of shear stresses

$$\begin{bmatrix} \frac{1}{Eh} & \frac{-\mu hv}{Eh} & \frac{-\mu hh}{Eh} & 0 & 0 & 0 \\ \frac{-\mu hv}{Eh} & \frac{1}{Ev} & \frac{-\mu hv}{Eh} & 0 & 0 & 0 \\ \frac{-\mu hh}{En} & \frac{-\mu hv}{En} & \frac{1}{Eh} & 0 & 0 & 0 \\ 0 & 0 & 0 & \frac{1}{Ghv} & 0 & 0 \\ 0 & 0 & 0 & 0 & \frac{1}{Ghv} & 0 \\ 0 & 0 & 0 & 0 & 0 & \frac{2(1+\mu hh)}{En} \end{bmatrix} \bullet \begin{Bmatrix} \sigma h \\ \sigma v \\ \sigma h \\ \tau hv \\ \tau vh \\ \tau hh \end{Bmatrix} = \begin{Bmatrix} \epsilon h \\ \epsilon v \\ \epsilon h \\ \gamma hv \\ \gamma vh \\ \gamma hh \end{Bmatrix}$$

Figure 1.3 Cross-anisotropic soil requiring results from more than triaxial tests for full characterization.

specimen such that uniform strains and stresses and therefore correct soil response can be produced. This is discussed in Chapter 3. In addition to the limitations listed above, it should be mentioned that it may be easier to reproduce certain stress paths in other specialty equipment than in the triaxial apparatus (e.g., K_0-test).

Although the triaxial test is limited as explained under points 2 and 3 above, it does combine versatility with relative simplicity in concept and performance. Other equipment in which three unequal principal stresses can be applied or in which the principal stress directions can be rotated do not have the versatility or is more complicated to operate. Thus, other types of equipment have their own advantages and limitations. These other equipment types include plane strain, true triaxial, simple shear, directional shear, and torsion shear apparatus. All these pieces of equipment are, with the exception of the simple shear apparatus, employed mainly for research purposes. Their operational modes, capabilities and results are reviewed in Chapter 11.

1.5 Test stages – consolidation and shearing

Laboratory tests are made to simulate field loading conditions as close as possible. Most field conditions and the corresponding tests can be simplified to consist of two stages: consolidation and shearing.

1.5.1 Consolidation

In the first stage the initial condition of the soil is established in terms of effective stresses and stress history (including overconsolidation, if applicable). Thus, stresses are applied corresponding to those acting on the element of soil in the field due to weight of the overlying soil strata and other materials or structures that exist at the time the mechanical properties (stress–strain, strength, etc.) are sought. Sufficient time is allowed for complete consolidation to occur under the applied stresses. The condition in the field element has now been established in the triaxial specimen.

1.5.2 Shearing

In the second stage of the triaxial test an additional stress is applied to reach peak failure and beyond under relevant drainage conditions. The additional stress applied to the specimen should correspond as closely as possible to the change in stress on the field element due to some new change in the overall field loading situation. This change may consist of a vertical stress increase or decrease (e.g., due to addition of a structure or excavation of overlying soil strata) or of a horizontal stress increase or decrease (e.g., due to the same constructions causing the vertical stress changes). Any combination of vertical and horizontal stress changes may be simulated in the triaxial test. Examples of vertical and horizontal stress changes in the field are shown in Fig. 1.4.

Usually, it is desirable to know how much change in load the soil can sustain without failing and how much deformation will occur under normal working conditions. The test is therefore usually continued to find the strength of the soil under the appropriate loading conditions. The results are used with an appropriate factor of safety so that normal working stresses are always somewhat below the peak strength.

The stress–strain relations obtained from the triaxial tests provide the basis for determination of deformations in the field. This may be done in a simplified manner by closed-form solutions or it may be done by employing the results of the triaxial tests for calibration of a constitutive model used with a numerical method in finite element or finite difference computer programs.

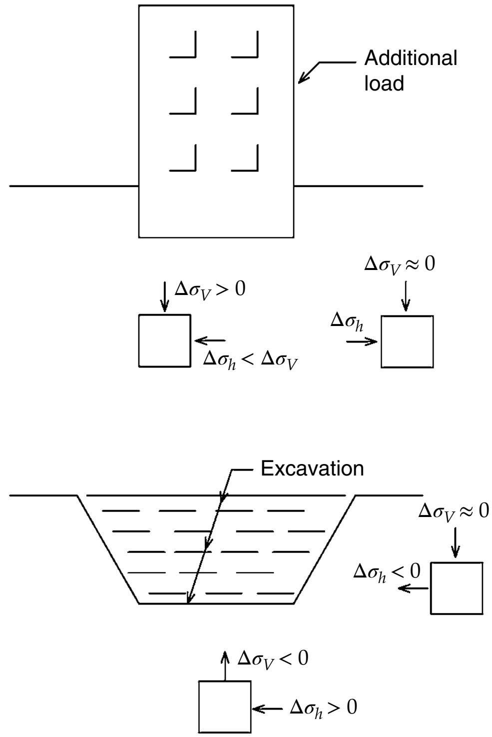

Figure 1.4 Examples of stress changes leading to failure in the field.

1.6 Types of tests

The drainage conditions in the field must be duplicated as well as possible in the laboratory tests. This may be done by appropriate drainage facilities or preventions as discussed above for the triaxial test. In most cases the field drainage conditions can be approximated by one of the following three types of tests:

1. Consolidated-drained test, called a CD-test, or just a drained test
2. Consolidated-undrained test, or a CU-test
3. Unconsolidated-undrained test, or a UU-test

These tests are described in ASTM Standards D7181 (2014), D4767 (2014), and D2850 (2014), respectively.

Which condition of drainage in the laboratory test logically corresponds to each case in the field depends on a comparison of loading rate with the rate at which the water can escape or be sucked into the ground. Thus, the permeability of the soil and the drainage boundary conditions in the field together with the loading rate play key roles in determination of the type of analysis and the type of test, drained or undrained, that are appropriate for each case. Field cases with partial drainage can be correctly duplicated in laboratory tests if the effective stress path is determined for the design condition. However, the idea of the CD-, CU- and UU-tests is to make it relatively simple for the design engineer to analyze a condition that will render a sufficient factor of safety under the actual drainage condition, without trying to estimate and experimentally replicate the actual stress path.

It has been determined through experience and common sense that the extreme conditions are drained and undrained with and without consolidation. As a practical matter, in a commercial laboratory it is easier to run an undrained test than a drained test because it is easier and faster to measure pore pressures than volume change. Therefore, even drained parameters are more likely to be estimated from a CU-test than from a CD-test.

1.6.1 Simulation of field conditions

Presented below is a brief review of the three types of tests together with examples of field cases for which the tests are appropriate and with typical strength results shown on Mohr diagrams.

Drained tests

Isotropic consolidation is most often used in the first stage of the triaxial test. However, anisotropic consolidation with any stress ratio is also possible.

The shearing stage of a drained test is performed so slowly, the soil is so permeable and the drainage facilities are such that no excess pore pressure (positive or negative) can exist in the specimen at any stage of the test, that is

$$\Delta u = 0 \tag{1.5}$$

It follows then from the effective stress principle

$$\sigma' = \sigma - u \tag{1.6}$$

that the effective stress changes are always the same as the total stress changes.

A soil specimen always changes volume during shearing in a drained test. If it contracts in volume, it expels pore fluid (usually water or air), and if it expands in volume (dilates), then it sucks water or air into the pores. If a non-zero pore pressure is generated during the test (e.g., by performing the shearing too fast so the water does not have sufficient time to escape), then the specimen will expel or suck water such that the pore pressure goes towards zero to try to achieve equilibrium between externally applied stresses and internal effective stresses. Thus, there will always be volume changes in a drained test. Consequently, the water content, the void ratio, and the dry density of the specimen at the end of the test are most often not the same as at the beginning.

The following field conditions can be simulated with acceptable accuracy in the drained test:

1. Almost all cases involving coarse sands and gravel, whether saturated or not (except if confined in e.g., a lens and/or exposed to rapid loading as in e.g., an earthquake).
2. Many cases involving fine sand and sometimes silt if the field loads are applied reasonable slowly.
3. Long term loading of any soil, as for example:
   a) Cut slopes several years after excavation
   b) Embankment constructed very slowly in layers over a soft clay deposit
   c) Earth dam with steady seepage
   d) Foundation on clay a long time after construction.

These cases are illustrated in Fig. 1.5.

The strength results obtained from drained tests are illustrated schematically on the Mohr diagram in Fig. 1.6. The shear strength of soils increases with increasing confining pressure.

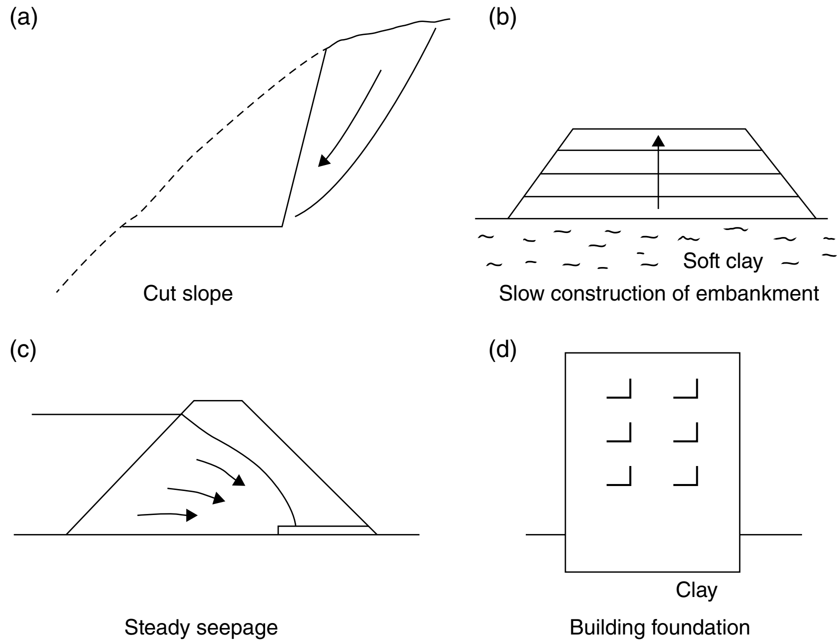

Figure 1.5 Examples of field cases for which long term stability may be determined on the basis of results from drained tests.

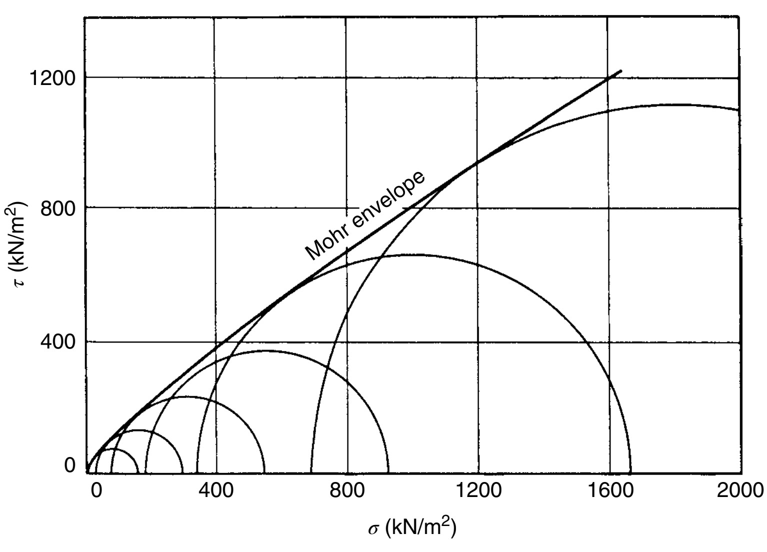

Figure 1.6 Schematic illustration of a Mohr diagram with failure envelope for drained tests on soil.

In the diagram in Fig. 1.6 the total stresses are equal to the effective stresses since there are no changes in pore pressures [Eqs (1.5) and (1.6)].

The effective friction angle, φ', decreases for all soils with increasing confining pressure, and the failure envelope is therefore curved, as indicated in Fig. 1.6. The effective cohesion, c', is zero or very small, even for overconsolidated clays. Effective or true cohesion of any significant magnitude is only present in cemented soils.

The effective stress failure envelope then defines the boundary between states of stress that can be reached in a soil element and states of stress that cannot be reached by the soil at its given dry density and water content.

Consolidated-undrained tests

As in drained tests, isotropic consolidation is most often used in CU-tests. However, anisotropic consolidation can also be applied, and it may have greater influence on the results from CU-tests than those from drained tests. The specimen is allowed to fully consolidate such that equilibrium has been obtained under the applied stresses and no excess pore pressure exists in the specimen.

The undrained shearing stage is begun by closing the drainage valve before shear loading is initiated. Thus, no drainage is permitted, and the tendency for volume change is reflected by a change in pore pressure, which may be measured by the transducer (see Fig. 1.2). Therefore the second stage of the CU-test on a saturated specimen is characterized by:

$$\Delta V = 0 \tag{1.7}$$

and

$$\Delta u \neq 0 \tag{1.8}$$

According to the effective stress principle in Eq. (1.6), the effective stresses are therefore different from the total stresses applied in a CU-test.

The pore pressure response is directly related to the tendency of the soil to change volume. This is illustrated in Fig. 1.7. Thus, there will always be pore pressure changes in an undrained test. However, since there are no volume changes of the fully saturated specimen, the water content, the void ratio and the dry density at the end of the test will be the same as at the end of the consolidation stage.

The following field conditions can be simulated with good accuracy in the CU-test:

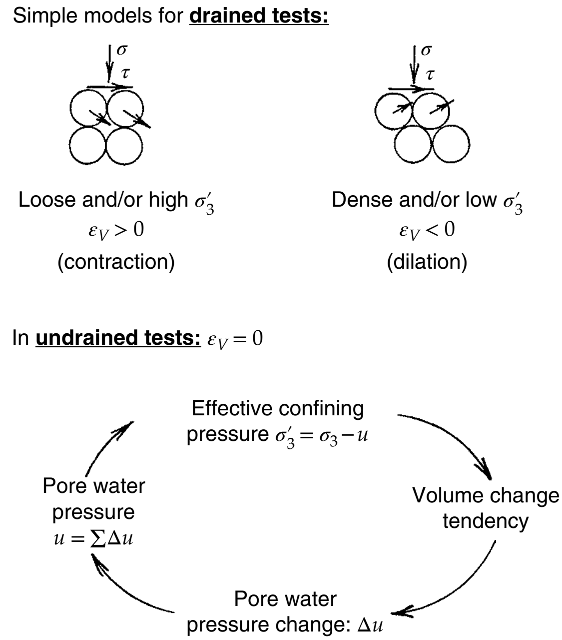

Figure 1.7 Schematic illustration of changes in pore water pressure in undrained tests.

1. Most cases involving short term strength, that is strength of relatively impervious soil deposits (clays and clayey soils) that are to be loaded over periods ranging from several days to several weeks (sometimes even years for very fat clays in massive deposits) following initial consolidation under existing stresses before loading. Examples of field cases in which short term stability considerations are appropriate:
   a) Building foundations
   b) Highway embankments, dams, highway foundations
   c) Earth dams during rapid drawdown (special considerations are required here, see Duncan and Wright 2005)These cases are illustrated in Fig. 1.8.
2. Prediction of strength variation with depth in a uniform soil deposit from which samples can only be retrieved near the ground surface. This is illustrated in Fig. 1.9.

The strength results obtained from CU-tests are illustrated schematically on the Mohr diagram in Fig. 1.10. Since pore pressures develop in CU-tests, two types of strengths can be derived from undrained tests: total strength; and effective strength. The Mohr circles corresponding to

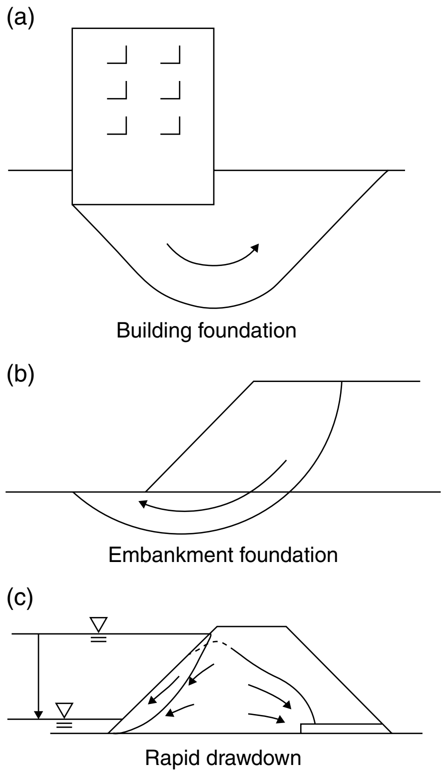

Figure 1.8 Examples of field cases for which short term stability may be determined on the basis of results of CU-tests.

these two strengths will always have the same diameter, but they are displaced by Δu from each other.

Both the total and effective stress envelopes from CU-tests on clays and clayey soils indicate increasing strength with increasing confining pressure. As for the drained tests, the effective friction angle, φ', decreases with increasing confining pressure, and the curvature of the failure envelope is sometimes more pronounced than for sands. In fact, the effective strength envelope obtained from CU-tests is very similar to that obtained from drained tests. Thus, the effective cohesion, c', is zero except for cemented soils. In particular, the effective cohesion is zero for remolded or compacted soils.

The total stress friction angle, φ, is much lower than the effective stress friction angle, φ', whereas the total stress cohesion, c, can have a substantial magnitude. The total stress friction angle is not a friction angle in the same sense as the effective stress friction angle. In the latter case, φ' is a measure of the strength derived from the applied normal stress, while φ is a measure of the strength gained from the *consolidation* stress only. If, for example, the total stress parameters are applied in a slope stability calculation in which a surcharge is suddenly added, then the surcharge will contribute to the shear resistance in the analysis (which is incorrect) as well as to the driving force, because there is no distinction between the normal forces derived from consolidation stresses and those caused by the surcharge. A better approach would be to assign undrained shear strengths (s_u) based on the consolidation stress state by using an approach that involves s_u/σ_v'.

Unconsolidated-undrained tests

In the UU-test a confining pressure is first applied to the specimen and *no drainage* is allowed. In fact, UU-tests are most often performed in triaxial equipment without facilities for drainage. The soil has already been consolidated in the field, and the specimen is therefore considered to “contain” the mechanical properties that are present at the location in the ground where the sample was taken. Alternatively, the soil may consist of compacted fill whose undrained strength is required for stability analysis before any consolidation has occurred in the field.

The undrained shearing stage follows immediately after application of the confining pressure. The shear load is usually increased relatively fast until failure occurs. No drainage is permitted during shear. Thus, the volume change is zero for a saturated specimen and the pore pressure is different from zero, as indicated in Eqs (1.7) and (1.8). The pore pressure is not measured and only the total strength is obtained from this test.

Since there are no volume changes in a saturated specimen, the void ratio, the water content and the dry density at the end of the test will be the same as those in the ground.

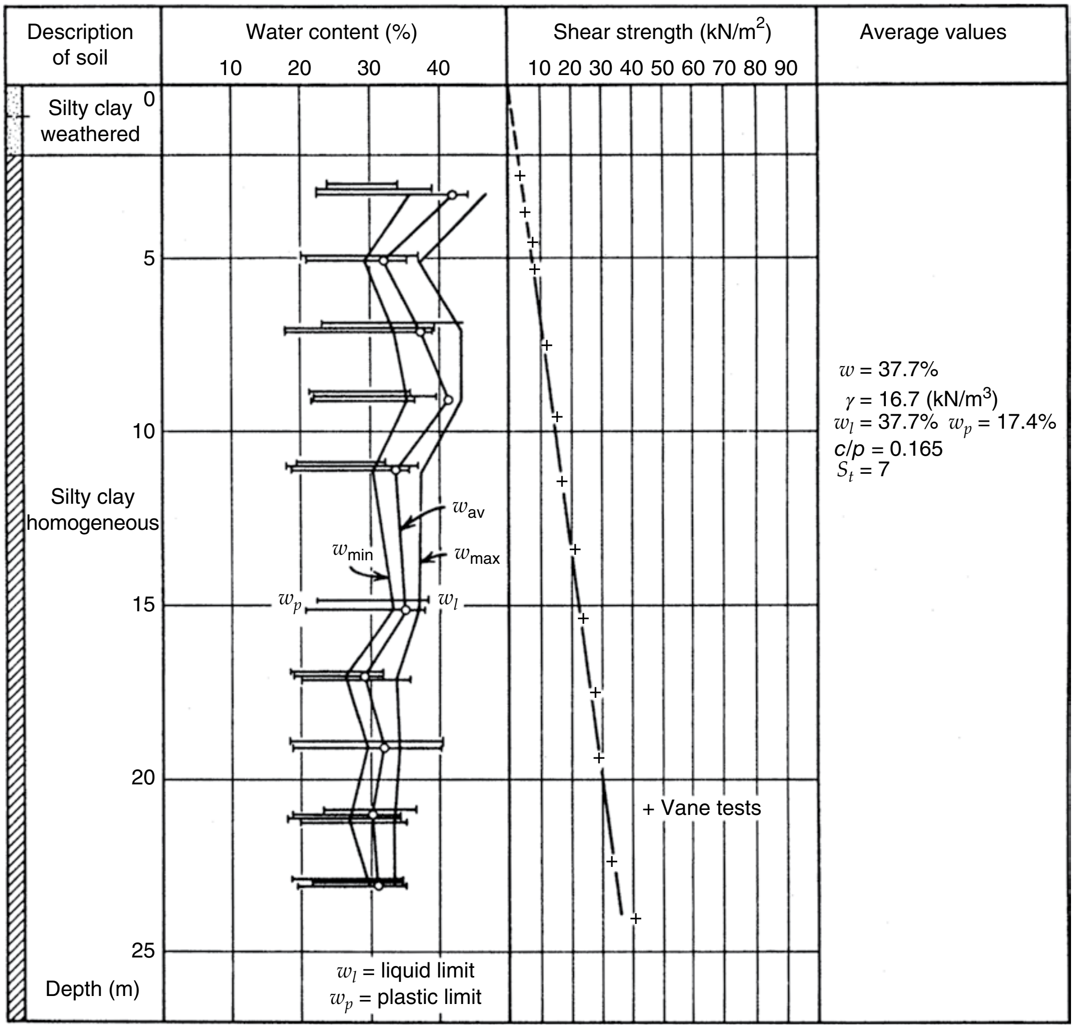

Figure 1.9 Strength variation with depth in uniform soil deposit of Norwegian marine clay. Reproduced from Bjerrum 1954 by permission of Geotechnique.

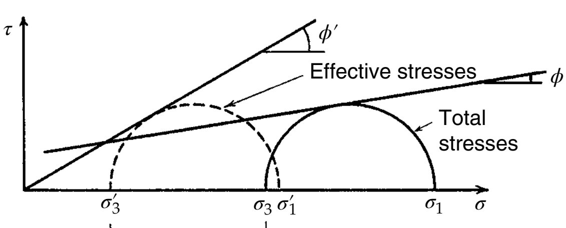

Figure 1.10 Schematic illustration of a Mohr diagram with total stress and effective stress failure envelopes from CU-tests on soil (after Bishop and Henkel 1962).

The following field conditions may be simulated in the UU-test:

1. Most cohesive soils of relatively poor drainage, where the field loads would be applied sufficiently rapidly that drainage does not occur. Examples of field cases for which results of UU-tests may be used:
   a) Compacted fill in an earth dam that is being constructed rapidly
   b) Strength of a foundation soil that will be loaded rapidly

c) Strength of soil in an excavation immediately after the cut is made

These cases are illustrated in Fig. 1.11.

2. Undisturbed, saturated soil, where a sample has been removed from depth, installed in a triaxial cell, and pressurized to simulate the overburden in the field.

The strength results obtained from UU-tests on *saturated* soil are illustrated schematically on the Mohr diagram in Fig. 1.12. The strength obtained from UU-tests on saturated soil is *not* affected by the magnitude of the confining pressure. This is because consolidation is not allowed after application of the confining pressure. Thus, the actual effective confining pressure in the saturated soil does not depend on the applied confining pressure, and the same strength is therefore obtained for all confining pressures. Consequently, the total strength envelope is horizontal corresponding to $\varphi = 0$, and the strength is therefore characterized by the undrained shear strength:

$$s_u = \frac{1}{2}(\sigma_1 - \sigma_3) \tag{1.9}$$

This is indicated in Fig. 1.12.

Since the UU-strength of a *saturated* soil is unaffected by the confining pressure, a UU-test may be performed in the unconfined state. This test is referred to as an unconfined compression test. In order that the unconfined compression test produces the same strength as would be obtained from a conventional UU-test, the soil must be:

1. Saturated
2. Intact
3. Homogeneous

Soils such as partly saturated clay (not saturated), stiff-fissured clays (not intact, fissures may open when unconfined), and varved clays (not homogeneous, cannot hold tension in pore water) do not fulfill these requirements

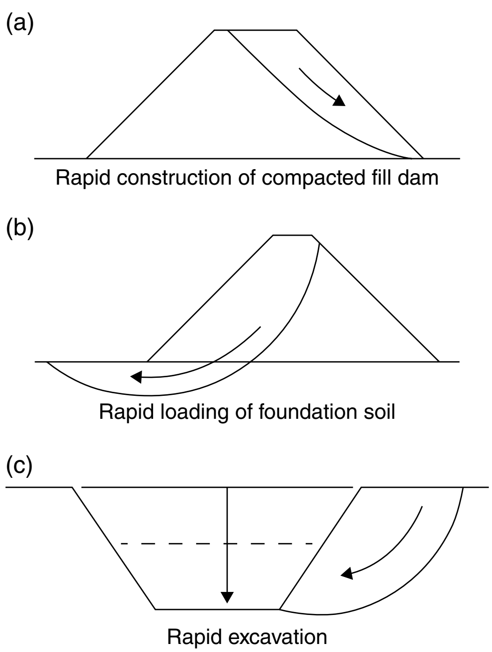

Figure 1.11 Examples of field cases for which short term stability may be determined on the basis of results of UU-tests.

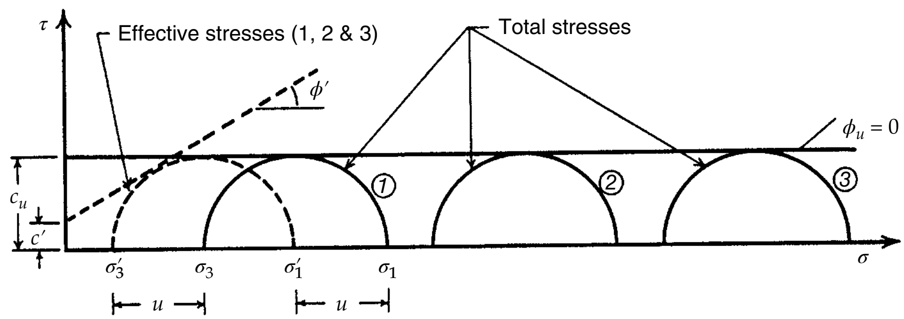

Figure 1.12 Schematic illustration of a Mohr diagram with results of UU-tests on saturated soil (after Bishop and Henkel 1962).

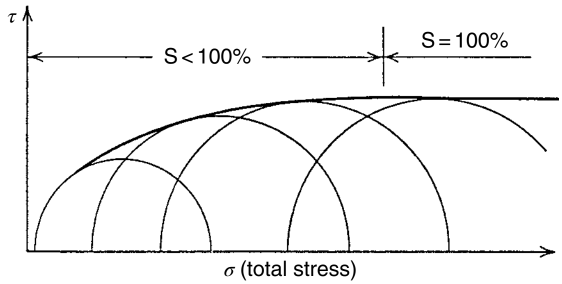

Figure 1.13 Schematic illustration of strength of partly saturated soil obtained from UU-tests.

and should not be tested in the unconfined compression test.

For those soils which qualify for and are tested in the unconfined compression test, the undrained *shear strength* is:

$$s_u = \frac{1}{2} \cdot q_u \tag{1.10}$$

in which q_u is the unconfined *compressive strength*:

$$q_u = (\sigma_1 - \sigma_3)_{\max} = \sigma_{1\max} \tag{1.11}$$

This is also indicated in Fig. 1.12.

For partly saturated soils the Mohr failure envelope is curved at low confining pressures, as seen in Fig. 1.13. As the air voids compress with increasing confinement, the envelope continues to become flatter. When all air is dissolved in the pore water, the specimen is completely saturated, and the envelope becomes horizontal. The undrained shear strength obtained at full saturation depends on the initial degree of saturation.

1.6.2 Selection of test type

The application of soil properties in analyses of actual geotechnical problems are outside the scope of the present treatment. However, it is important to know in which type of analysis the soil properties are to be used before any testing is initiated. Thus, different types of analyses (total stress or effective stress, short term or long term) may require results from different types of tests or results from different methods of interpretation of the results. In other words, the analysis that is appropriate for each particular field condition dictates the type of triaxial test to be performed.

Generally, soils that tend to contract will develop positive pore pressures during undrained shear resulting in lower shear strength than that obtained from the corresponding drained condition. Short term stability involving undrained conditions would be most critical for such soils. On the other hand, soils that tend to dilate will develop negative pore pressures during undrained shear resulting in higher shear strength than that obtained from the corresponding drained condition. Long term stability involving drained behavior would be most critical for these soils. Field conditions involving partial drainage should be analyzed for the most critical condition(s). For example, an earth dam usually undergoes several different stability analyses corresponding to different phases of construction and operating conditions. Some guidelines may be obtained from the examples given above.

2 Computations and Presentation of Test Results

2.1 Data reduction

Reduction of measured quantities in element tests, such as the triaxial compression test, involves computation of strains, cross-sectional areas, and stresses. Corrections to these quantities may be required to obtain the true behavior of the soil. Corrections to measurements are reviewed in Chapter 9.

2.1.1 Sign rule – 2D

The sign rule employed in soil mechanics has traditionally been opposite to that used in other branches of mechanics in which tensile stress and strains are considered to be positive. This is because most soils exhibit negligible tensile strengths and because deformation and failure most often are produced in response to compressive stresses. To avoid calculations in which the majority of quantities are negative, it is convenient to employ a sign rule in which compressive, normal stresses and strains are positive, as illustrated in Fig. 2.1(a) and (b). This requires a corresponding change in signs for shear stresses and shear strains. Figure 2.1(c) and (d) shows that shear stresses and strains are positive when acting in the counterclockwise direction under two-dimensional (2D) conditions.

As a consequence of this sign rule, the volumetric strains are positive for compression or contraction and negative for expansion or dilation. Thus, the loss of volume in a soil element results in a positive volumetric increment. This may not seem immediately logical, but it is necessary for consistency in the strain computations.

2.1.2 Strains

The strains in a soil element such as a triaxial specimen are calculated from the measured linear and volumetric deformations. Assuming these deformations to be uniformly distributed within the specimen, the strains may be calculated with reference to the original specimen dimensions resulting in "conventional" or "engineering" strains, or they may be calculated with reference to the current dimensions in which case they are referred to as "natural," "logarithmic," or "true" strains.

Engineering strains

The definition of engineering strains is most often employed in soil mechanics. The engineering strains may be converted to natural strains as shown below.

The linear engineering strains of a prismatic volume element with initial side lengths of L_1,

Triaxial Testing of Soils, First Edition. Poul V. Lade.

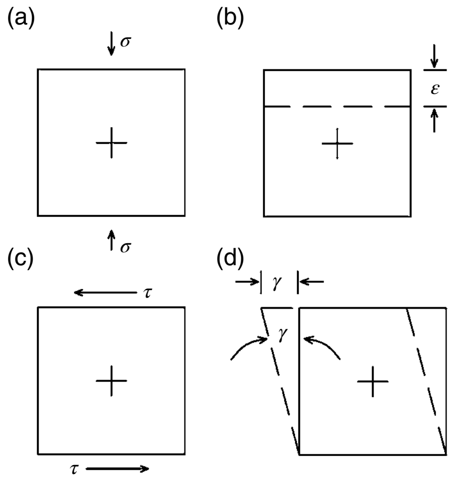

Figure 2.1 Sign rule employed in soil mechanics: compressive normal (a) stresses, σ, and (b) strains, ε, are positive. Shear (c) stresses, τ, and (d) strains, γ, are positive when directed counterclockwise (in two dimensions).

L_2, and L_3 and with incremental changes in these side lengths of ΔL_1, ΔL_2, and ΔL_3 are defined as:

$$\varepsilon_1 = \frac{\Delta L_1}{L_1} \tag{2.1}$$

$$\varepsilon_2 = \frac{\Delta L_2}{L_2} \tag{2.2}$$

$$\varepsilon_3 = \frac{\Delta L_3}{L_3} \tag{2.3}$$

and the volumetric strain of the element, whose initial volume is $V_0 = L_1 \cdot L_2 \cdot L_3$, is calculated from the volume change ΔV as follows:

$$\varepsilon_v = \frac{\Delta V}{V_0} \tag{2.4}$$

The relation between linear and volumetric strains may be derived by expressing the current volume in terms of the current linear dimensions:

$$V_0 - \Delta V = (L_1 - \Delta L_1)(L_2 - \Delta L_2)(L_3 - \Delta L_3) \tag{2.5}$$

Division by $V_0 = L_1 \cdot L_2 \cdot L_3$ and substitution of the expressions for the linear and volumetric strains produces the following relation for a unit volume:

$$1 - \varepsilon_v = (1 - \varepsilon_1)(1 - \varepsilon_2)(1 - \varepsilon_3) \tag{2.6}$$

Further reduction yields a general relation between the strains:

$$\varepsilon_v = \varepsilon_1 + \varepsilon_2 + \varepsilon_3 - \varepsilon_1 \cdot \varepsilon_2 - \varepsilon_2 \cdot \varepsilon_3 - \varepsilon_3 \cdot \varepsilon_1 + \varepsilon_1 \cdot \varepsilon_2 \cdot \varepsilon_3 \tag{2.7}$$

The physical meaning of the terms in Eq. (2.7) is illustrated in Fig. 2.2 for a prismatic element whose initial volume is unity (V_0 = 1) and which has undergone contraction in all three perpendicular directions. By adding and subtracting the effects of the linear strains (the three entire slabs), the products of two linear strains (the full lengths of the three bars), and the product of the three linear strains (the small prism), the relation between volumetric and linear strains given in Eq. (2.7) is obtained.

The expression in Eq. (2.7) accounts correctly for the relation between linear and volumetric strains whether these are positive or negative, and it may be used for small as well as large strains. For small strains the second and third order terms become small and may be neglected. Thus, for *small strains* the following expression may be employed:

$$\varepsilon_v = \varepsilon_1 + \varepsilon_2 + \varepsilon_3 \tag{2.8}$$

Using this expression for calculations involving large strains may produce errors whose magnitudes and significance will be considered below.

Natural strains

The definition of "natural" strain was introduced by Ludwik (1909) to obtain a measure of strain with reference to the current dimension of an element undergoing deformations. Thus, the increment in strain referred to the current length is defined as (considering the sign rule in soil mechanics):

$$d\bar{\varepsilon} = -\frac{dL}{L} \tag{2.9}$$

and the total natural strain, $\bar{\varepsilon}$, obtained from the initial length L_0 to the length L is:

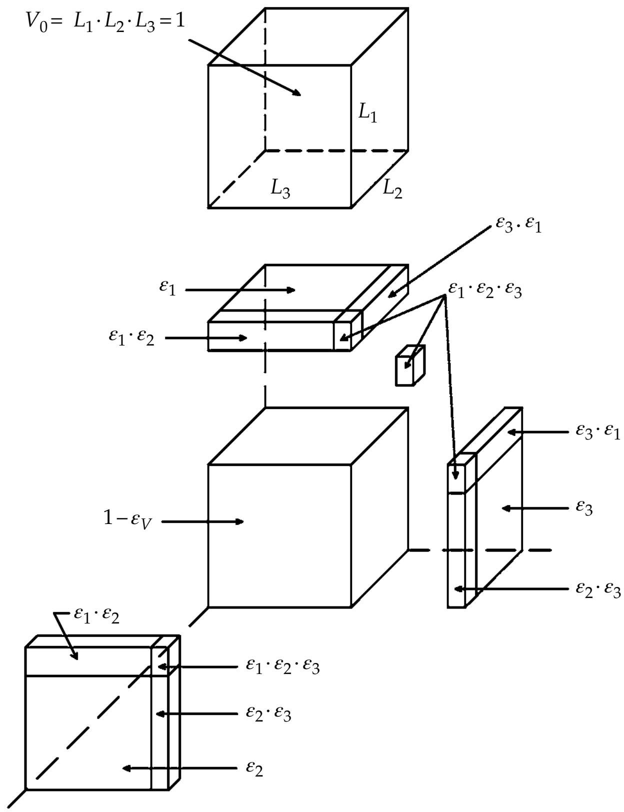

Figure 2.2 Spatial representation of strains in three dimensions.

$$\bar{\varepsilon} = -\int_{L_0}^{L} \frac{dL}{L} = -\ln\left(\frac{L}{L_0}\right) \tag{2.10}$$

This measure of strain represents an average strain obtained during deformation from L_0 to L. Its relation to engineering strain, ε, is readily determined since:

$$\frac{L}{L_0} = \frac{L_0 - \Delta L}{L_0} = 1 - \varepsilon \tag{2.11}$$

and therefore:

$$\bar{\varepsilon} = -\ln(1-\varepsilon) \tag{2.12}$$

Since the engineering strain, ε, is positive for contraction, the natural strain, $\bar{\varepsilon}$, is also positive for contraction, as indicated by Eq. (2.12). For small strains the engineering and the natural strains are practically identical. The natural strains have the advantage of being additive, whereas the engineering strains are not. Taking the natural logarithm on both sides of Eq. (2.6) results in the following simple expression for the natural volumetric strain:

$$\bar{\varepsilon}_v = \bar{\varepsilon}_1 + \bar{\varepsilon}_2 + \bar{\varepsilon}_3 \tag{2.13}$$

This expression is correct for small as well as for large strains. The comparable expression in Eq. (2.8) for engineering strains is correct only for small strains.

Although there are advantages associated with the natural strain definition, engineering strains are most often employed in practice and these will be used in the following.

Strains in a triaxial specimen

The engineering strains in a triaxial specimen are assumed to be uniform and may be calculated assuming the cylindrical specimen deforms as a right cylinder. For isotropic or cross-anisotropic materials with the axis of rotational symmetry in the vertical direction, the two radial, normal strains are equal. For these conditions the linear and volumetric strains are calculated as follows:

$$\text{Axial strain:} \quad \varepsilon_a = \frac{\Delta H}{H_0} \quad (= \varepsilon_1 \text{ for triaxial compression}) \tag{2.14}$$

$$\text{Radial strain:} \quad \varepsilon_r = \frac{\Delta D}{D_0} \quad (= \varepsilon_2 = \varepsilon_3 \text{ for triaxial compression}) \tag{2.15}$$

$$\text{Volumetric strain:} \quad \varepsilon_v = \frac{\Delta V}{V_0} \tag{2.16}$$

in which ΔH, ΔD, and ΔV are the increments and H_0, D_0, and V_0 are the initial height, diameter, and volume, respectively. For this axisymmetric condition, the two perpendicular, radial strains are equal, $\varepsilon_r = \varepsilon_2 = \varepsilon_3$. In a triaxial *compression* test, in which $\sigma_1 > \sigma_2 = \sigma_3$, the axial strain is the major principal strain (positive) and the radial strains are the minor principal strains (negative), as indicated in Eqs (2.14) and (2.15). In a triaxial *extension* test, in which $\sigma_1 < \sigma_2 = \sigma_3$, the axial strain is the minor principal strain (negative) and the radial strains are the major principal strains (positive).

The axial and volumetric strains are most often the basis for calculation of the radial strain as well as the cross-sectional area of the specimen. Setting $\varepsilon_2 = \varepsilon_3 = \varepsilon_r$ in the expression for volumetric strains in Eq. (2.7) produces an expression for ε_r which is valid for small as well as for *large strains*:

$$\varepsilon_r = 1 - \sqrt{\frac{1-\varepsilon_v}{1-\varepsilon_a}} \quad (= \varepsilon_3 \text{ for triaxial compression}) \tag{2.17}$$

The volumetric strain expression in Eq. (2.8) yields a simpler equation for the radial strain which is only valid for *small strains*:

$$\varepsilon_r = \frac{1}{2}(\varepsilon_v - \varepsilon_a) \quad (= \varepsilon_3 \text{ for triaxial compression}) \tag{2.18}$$

These expressions are valid for both compression and extension tests.

Evaluation of small strain calculations

It is convenient to use the small strain expressions in Eqs (2.8) and (2.18) for data reduction, and these expressions are most often employed in practice. The accuracy these expressions provide may be evaluated for various types of axisymmetric test conditions encountered in triaxial testing. To illustrate the difference between the two expressions for the radial strains, the following conditions, often experienced in soil testing, are considered: (1) isotropic compression and expansion of an isotropic material in which the three linear strains are equal; and (2) undrained compression and extension of triaxial specimens in which the volumetric strains are zero.

The diagram in Fig. 2.3 shows the difference between calculated radial strains from Eqs (2.17) and (2.18). The correct volumetric strains

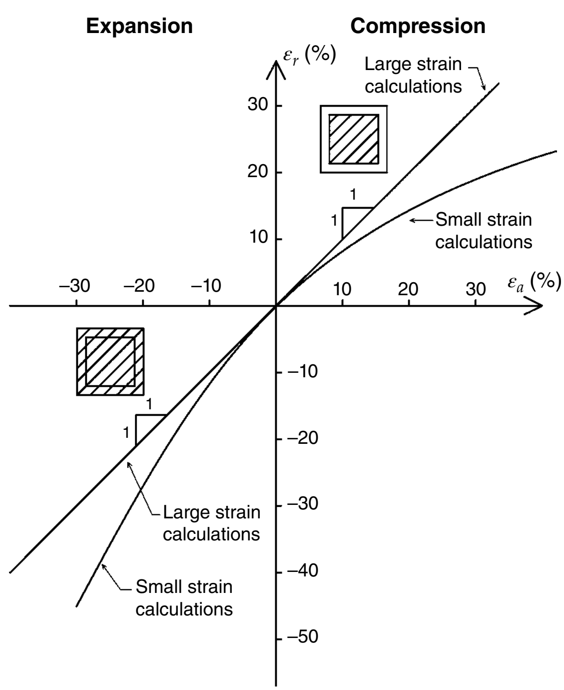

Figure 2.3 Comparison of radial strains calculated from axial and volumetric strains for isotropic compression and expansion of isotropic material.

are obtained from Eq. (2.7) and used in the expressions. The large strain calculations produce the correct radial strains for the isotropic material. The small strain calculations produce radial strains that are too small, whether contraction or expansion. The error is about 1.5% at ±10% axial strain, and it increases to 12% for contraction and 15% for expansion at axial strains of ±30%. In most cases of isotropic contraction and expansion of soil specimens, the linear strains are limited to much smaller values, and the small strain calculations may be sufficiently accurate for practical purposes.

Figure 2.4 shows the radial strains calculated for undrained compression and extension tests on specimens with zero volumetric strains. The large strain calculations produce the correct radial strains. The small strain calculations produce radial strains which, for the compression test indicate too little expansion, and for the extension test show too much contraction. The error is about 0.4% at 10% contraction, and it increases to 4.5% at 30% contraction. For extension, the error is about 0.35% at −10% axial strain, and it increases to 2.7% at −30% axial strain. The axial strain-to-failure is often much smaller in extension than in compression, and the small strain calculations may be sufficiently accurate for extension tests. The axial strain-to-failure is largest in triaxial compression tests (as compared with any other test condition in which the principal stresses are fixed in direction, see also Chapter 11), and it may therefore involve too large inaccuracies to use the small strain calculations for such tests.

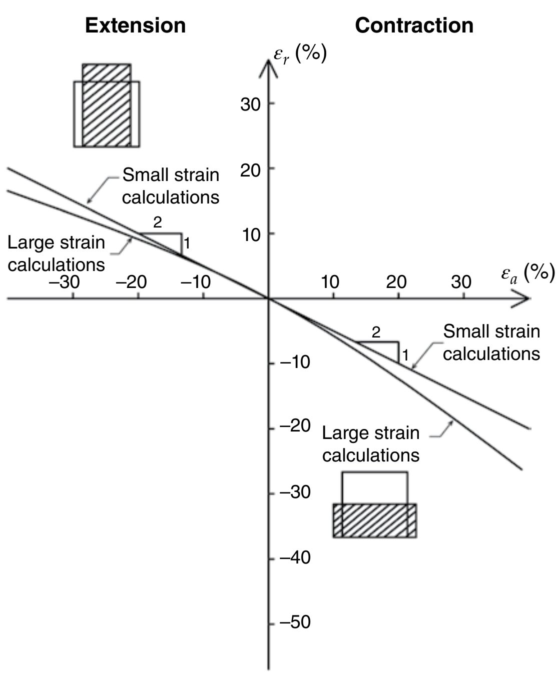

Figure 2.4 Comparison of radial strains calculated from axial and volumetric strains for undrained compression and extension specimens with zero volume change.

Note that if shear banding occurs the strain calculations are no longer valid, because all of the deformation occurs in the shear band.

An overall evaluation of the errors in radial strains produced by small strain calculations for various axisymmetric test conditions is illustrated in Fig. 2.5. In this diagram the initial shape and volume is indicated by a square for each test condition. The deformed shapes are shown by shaded squares or rectangles. Small strain calculations lead to correct radial strains for uniaxial strain or K_0-conditions only. The relative magnitude of errors in all other cases may be evaluated by comparing individual test conditions with those in Fig. 2.5. An indication of the absolute magnitude of errors may be obtained by reference to Figs 2.3 and 2.4.

Because computers or programmable calculators are often employed, the large strain expressions for the volumetric and radial strains in Eqs (2.7) and (2.17) may as well be used for data reduction with resulting greater accuracy in the calculated strains.

Soils with anisotropic behavior

The triaxial test may be used to determine anisotropic soil behavior only for cases in which one of the three axes of material symmetry is aligned with the vertical axis of the triaxial apparatus. For a cross-anisotropic material this includes two possible orientations, and for a material with general anisotropy, three different orientations are possible. These orientations are indicated in Fig. 2.6.

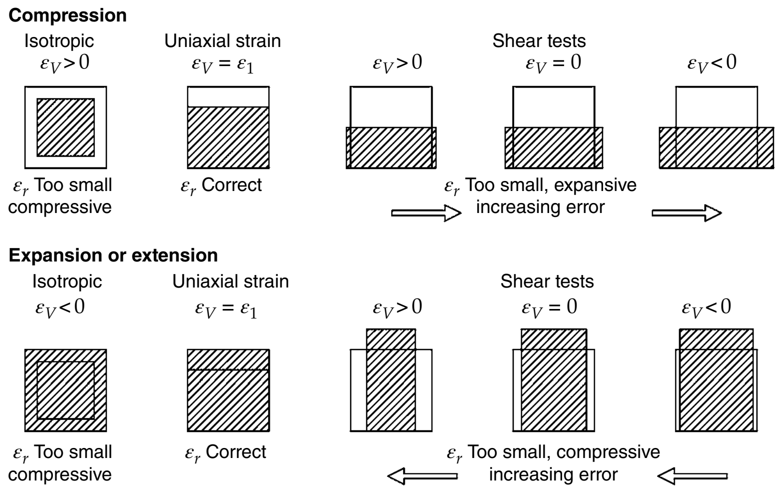

Figure 2.5 Evaluation of errors in radial strains calculated from axial and volumetric strains using small strain calculations.

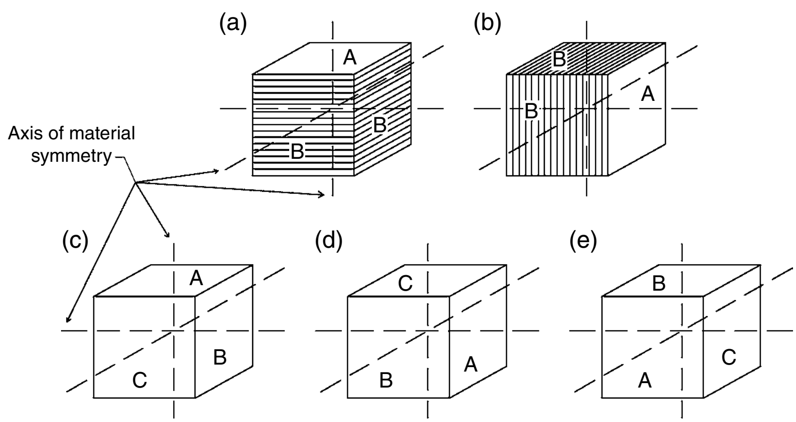

Figure 2.6 Possible orientations in triaxial apparatus of specimens with (a) and (b) cross-anisotropic material and (c), (d) and (e) general anisotropic material.

Except for the specimen in Fig. 2.6(a), the lateral strains in specimens with anisotropic behavior are expected to be different. To determine these lateral strains, it is necessary to measure the deformation in at least one lateral direction. This produces one lateral strain (say ε_2), and the other lateral strain (say ε_3) may be calculated from the expression in Eq. (2.7) as follows:

$$\varepsilon_3 = \frac{\varepsilon_v - \varepsilon_1 - \varepsilon_2 + \varepsilon_1 \cdot \varepsilon_2}{1 - \varepsilon_1 - \varepsilon_2 + \varepsilon_1 \cdot \varepsilon_2} \tag{2.19}$$

in which ε_1 and ε_v are the measured vertical and volumetric strains, respectively. For small strains Eq. (2.8) produces a simple expression for the unknown lateral strain:

$$\varepsilon_3 = \varepsilon_v - \varepsilon_1 - \varepsilon_2 \tag{2.20}$$

Alternatively, both lateral deformations may be measured, and Eq. (2.7) provides a check on the accuracy of the measurements.

Caution

Strains as well as stresses in triaxial tests on specimens prepared with axes of material symmetry inclined relative to the vertical axis of the apparatus are nonuniform and difficult to interpret correctly. Figure 2.7(a) and (b) shows

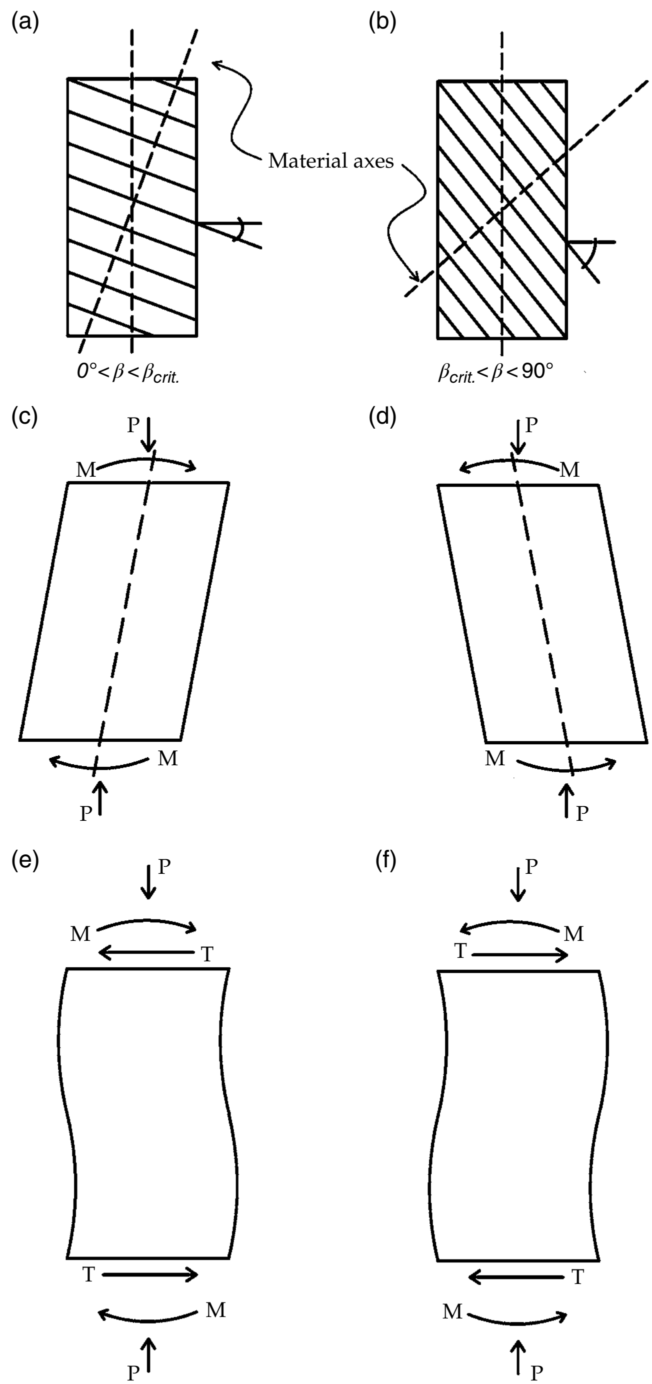

Figure 2.7 Schematic illustration of tests on specimens with inclined material axes. (a) and (b) initial vertical specimens, (c) and (d) deformed shapes of specimens with lubricated ends, and (e) and (f) deformed shapes of specimens with end restraint.

prismatic specimens with inclined bedding planes. For the ideal case in which only normal stresses are applied by horizontal end plates (requiring smooth, lubricated ends), moments are generated at the ends in response to the shear strains developing along the bedding planes. The initially vertical specimen acquires the shape of a parallelogram, and the specimen axis becomes inclined, as shown in Fig. 2.7(c) and (d). The vertical, normal stress distributions at the ends become nonuniform, and the state of stress and the pore water pressures or the volume changes become nonuniform inside the specimen.

If, on the other hand, the deformations of the specimen are restrained at the ends (requiring end plates with full friction), bending moments and shear forces will develop at the ends, causing the specimen to deform nonuniformly, and the states of stress and strain inside the specimen are nonuniform. Typical shapes of the deformed specimens are shown in Fig. 2.7(e) and (f).

Whether the end plates have full friction or are provided with lubrication, triaxial tests on specimens with inclined material axes are at best difficult to interpret, and the results of such tests are questionable. More detailed studies and discussions of these types of tests have been presented by Saada (1970) and Saada and Bianchini (1977). To study the behavior of anisotropic materials it is preferable to incline the principal stress directions rather than incline the specimen. This may be done in equipment in which shear stresses can be applied to the surface of the specimen (see Chapter 11).

Effects of bulging

Triaxial compression specimens with end restraint often exhibit nonuniform deformations during shear. Rather than deforming as a right cylinder, the specimen may bulge at the middle and attain the shape of a barrel. This mode of deformation is particularly pronounced for soils that contract during shear. Vertical, lateral, and volumetric strain distributions as well as the stress distribution inside the specimen become nonuniform, and interpretation of test results are consequently complicated. Although the external shape of the specimen may not indicate the true internal strain distribution, due to conically shaped dead zones near the end plates (for further discussion see Chapter 3), the effects of bulging on the average lateral and vertical strains under various conditions of end restraint may be studied.

Lateral strain distribution

The profile of the barrel-shaped specimen may be described with good approximation as a parabola, as indicated in Fig. 2.8. The following simple analysis indicates the magnitude of nonuniformity in the lateral strain distribution.

For full fixity at the ends, the two shaded areas in Fig. 2.8 are equal. The calculations shown on this figure indicate that the maximum lateral strain at the middle of the bulged specimen is 50% larger than the average lateral strain obtained from the deformed right cylinder. If some lateral deformation occurs at the ends, the nonuniformity decreases, and complete uniformity in lateral strain is obtained when the specimen deforms as a right cylinder.

Average lateral strains

The points at which the parabolic barrel crosses the deformed right cylinder may be obtained by analysis of the parabolic curve in the X–Y coordinate system shown in Fig. 2.8. The results shown in this figure indicate that the crossover points occur at approximately one-fifth of the specimen height from the end plates. The locations of these points are independent of the amount of restraint at the ends. Thus, if some lateral deformation occurs at the ends, the crossover points remain at the same location.

Based on this simple analysis, the average lateral deformation in a specimen that bulges may be measured at the points located one-fifth of the specimen height from the end plates. If measurements of the lateral deformations are performed directly on the cylindrical specimen (see also Chapter 4), and the average lateral deformations are sought, the measurement devices should be attached to the specimen at

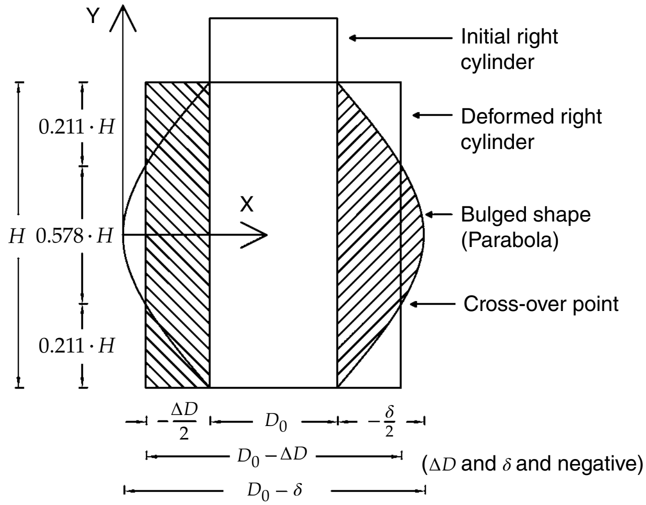

Area of shaded rectangle = area of shaded parabola section

$$H\cdot\left(-\frac{\Delta D}{2}\right)=\frac{2}{3}\cdot H\cdot\left(-\frac{\delta}{2}\right)$$

$$\delta=\frac{3}{2}\cdot\Delta D$$

Expression for parabola: $Y^2=R\cdot X$

At ends: $Y=\pm\frac{H}{2}$ *at* $X=-\frac{3}{4}\cdot\Delta D$

$$R=\frac{Y^2}{X}=\frac{\left(\frac{H}{2}\right)^2}{\left(-\frac{3}{4}\cdot\Delta D\right)}=\frac{H^2}{-3\Delta D}$$

Cross-over point @

$$X=-\frac{\delta}{2}-\frac{\Delta D}{2}=-\frac{1}{4}\cdot\Delta D$$

$$Y^2=\frac{H^2}{(-3\Delta D)}\cdot\left(-\frac{1}{4}\cdot\Delta D\right)\ \frac{H^2}{12}$$

$$Y=\pm\frac{\sqrt{3}}{6}\cdot H=\pm 0.289\cdot H$$

Figure 2.8 Analysis of deformations in a barrel-shaped specimen.

these points. Even if lubricated ends are employed and the specimen is believed to deform uniformly, it may be good practice to use these points for measurements.

In extension tests with end restraint, the deformed shape of the specimen resembles a paraboloid whose profile may also be approximated by a parabolic curve. The analysis of the deformed shape then proceeds as indicated above and similar results are obtained. Thus, full friction at the ends results in contractive lateral strains at the middle of the specimen which are 50% larger than the average lateral strains. The points located one-fifth of the specimen height from the ends may be used to obtain the average lateral deformations of triaxial specimens. Note however that for comparable compression and extension tests the strain to peak failure is usually much lower in extension. The parabolic shape of the profile is therefore not likely to be nearly as pronounced in extension as in compression. Further, necking and shear planes tend to develop at an early stage in conventional extension tests, thus invalidating the assumption of the parabolic shape. Conventional extension tests have been shown to be highly unstable and almost always result in erroneous stress–strain and strength results (Yamamuro and Lade 1995; Lade *et al*. 1996). See also below, and Chapter 10.

Vertical strain distribution

The vertical strain distribution is not as clearly visible as the lateral strain distribution. However, measurements along the axis of compression specimens indicate that the vertical strain distribution may also be parabolic with the largest strains near the middle. Even for full fixity, the vertical strains at the ends are not zero, since vertical strains occur in uniaxial strain or K_0-tests. Approximate analyses of vertical strain distributions may, however, be performed in a similar manner as indicated above. The average vertical strain is obtained from measurement of the vertical deformation over the total height of the specimen.

Volumetric strain distribution

The distribution of volume changes follows the pattern indicated above for the linear strains. Due to end restraint the specimen is likely to contract least or dilate most near the middle. The overall volume change measured (e.g., by the amount of water expelled from or sucked into the specimen) represents the average volumetric strain.

Detailed measurements and analyses

The brief review of effects of bulging presented above used relatively simple analysis procedures based on parabolic shapes. More detailed measurements of strain distributions in triaxial specimens may be performed. Detailed analyses based on finite element calculations may also be evaluated.

Development of shear planes

Granular soils that tend to dilate as well as clays in which the platy particles tend to align during shear, with both effects resulting in lower strengths, may develop shear planes or bands when tested in triaxial compression or extension. Once one or more shear planes have initiated in specimens of sufficient height to allow their free development, the deformations become localized to the shear plane, and two essentially solid portions of the specimen move past each other along the shear plane. Figure 2.9 shows a triaxial compression specimen with a shear plane. Very large shear strains occur inside the shear plane, which, due to dilation in granular materials and particle alignment in clays, becomes a weak plane in the specimen. The strains in the specimen become highly non-uniform, and the true relation between stresses and strains cannot be determined from external measurements. The two large volumes of the

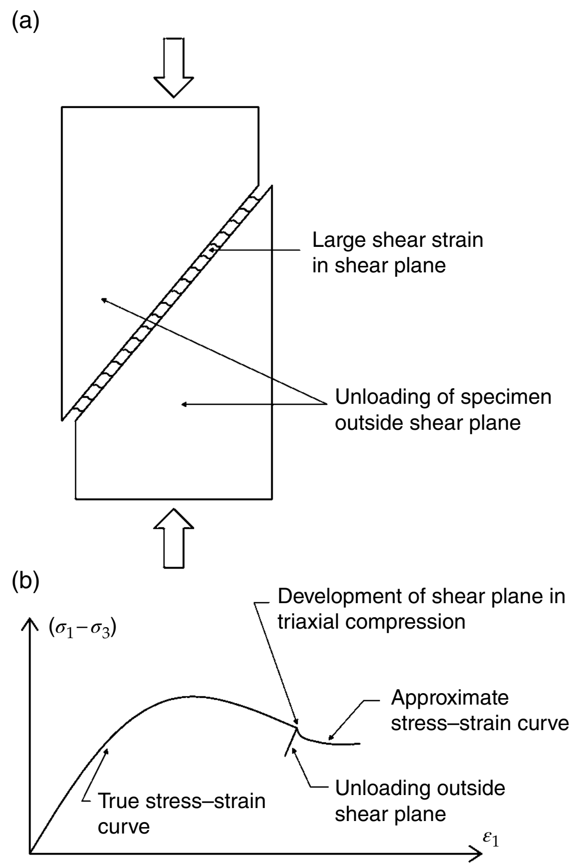

Figure 2.9 (a) Development of shear planes in a triaxial compression specimen and (b) the resulting stress–strain relationship.